interconversion and nearly no activation energy for small conformational change (e.g., C3'-exo <<*mr C2'-endo).[27,28] These calculations did not take account of crystalline packing or hydrogen bonding.

(27) Olson, W. K.; Sussman, J. L. *J. Am. Chem. Soc.* **1982**, *104*, 270-278.
(28) Olson, W. K. *J. Am. Chem. Soc.* **1982**, *104*, 278-286.

Acknowledgment. We thank Heisaburo Shindo for continuous encouragement with this work. We also thank Rolf Tschudin for his expert technical support.

Registry No. D_2, 7782-39-0; thymine-*methyl*-d_3, 68941-98-0; 2-deoxyribose 1-phosphate, 17039-17-7; thymidine-2',2'-d_2, 100447-82-3; thymidine, 50-89-5.

Hyperfine Interactions of ^{57}Fe in Human Transferrin: An ENDOR Spectroscopic Study

Gerald A. Rottman,[1a] Kei Doi,[1a] Olga Zak,[1a] Roland Aasa,[1b] and Philip Aisen*,[1a]

Contribution from the Department of Physiology and Biophysics, Albert Einstein College of Medicine, 1300 Morris Park Avenue, Bronx, New York 10461, and Department of Biochemistry and Biophysics, Chalmers University of Technology and University of Göteborg, S-412 96 Göteborg, Sweden. *Received May 15, 1989*

Abstract: Electron nuclear double resonance (ENDOR) spectra have been obtained for high-spin $^{57}Fe(III)$ complexes of human serum transferrin and ethylenebis[(*o*-hydroxyphenyl)glycine] (EHPG), a compound used to model the specific sites of transferrin. The pseudonuclear Zeeman effect (PNZE), representing interaction of electronic Zeeman and hyperfine terms of the spin Hamiltonian, is primarily responsible for splitting of ENDOR lines, the nuclear Zeeman term making a negligible contribution to line separation. The sensitivity of the PNZE to zero-field splittings makes it possible to extract fine structure as well as hyperfine parameters of the spin Hamiltonian from analysis of the ^{57}Fe ENDOR spectra. Differences between the two sites of transferrin are reflected in *D*, the axial parameter of the fine structure operator.

The study of hyperfine interactions by EPR spectroscopy has provided valuable information regarding the ligand structure of metal-binding sites in metalloproteins and the electronic configuration of the bound metal ions. Transferrin, a protein functioning in the transport and delivery of iron to cells, has been the subject of numerous spectroscopic studies probing the ligand structure of its two specific metal-binding sites. EPR, pulsed EPR, and electron nuclear double resonance (ENDOR) spectroscopies have been particularly productive in the study of the Cu(II) and VO^{2+} complexes of transferrin, revealing differences between the two sites,[2,3] the presence of a single histidyl nitrogen ligand,[4,5] the coordination to the metal ion of the synergistic anion required for metal binding,[5] and the accessibility of bound metal ion to solvent.[6] Despite these successes, details of hyperfine structure in the physiologically important Fe(III) complexes of transferrin have been elusive as they are obscured by relatively large line widths in the EPR spectra (>15 G).

We now report observation of hyperfine structure in ^{57}Fe-(III)-transferrin complex by means of electron nuclear double resonance spectroscopy. A computer fit of experimental data to an appropriate spin Hamiltonian has permitted determination of the hyperfine coupling and zero-field parameters in the protein's physiological iron-bearing state. Site-specific information was obtained by selectively loading one metal-binding site at a time with ^{57}Fe. Similar studies were carried out on ethylenebis[(*o*-hydroxyphenyl)glycine] (EHPG), a compound that has been used to model the Fe(III)-binding sites of transferrin.[7-10]

(1) (a) Albert Einstein College of Medicine. (b) Chalmers University of Technology and University of Göteborg.
(2) Zweier, J. L.; Aisen, P. *J. Biol. Chem.* **1977**, *252*, 6090.
(3) Chasteen, N. D.; White, L. K.; Campbell, R. F. *Biochemistry* **1977**, *16*, 363.
(4) Roberts, J. E.; Brown, T. G.; Hoffman, B. F.; Aisen, P. *Biochem. Biophys. Acta* **1983**, *747*, 49.
(5) Zweier, J. L.; Aisen, P.; Peisach, J.; Mims, W. B. *J. Biol. Chem.* **1979**, *254*, 3512.
(6) Zweier, J. L. *J. Biol. Chem.* **1980**, *255*, 2782.
(7) Gaber, B. P.; Miskowski, V.; Spiro, T. G. *J. Am. Chem. Soc.* **1974**, *96*, 6868.
(8) Pecoraro, V. L.; Harris, W. R.; Carrano, C. J.; Raymond, K. N. *Biochemistry* **1981**, *20*, 7033.
(9) Spartalian, K.; Carrano, C. J. *J. Chem. Phys.* **1983**, *78*, 4811.

Materials and Methods

Sample Preparation. Human serum transferrin was purchased from Calbiochem-Behring. Since this commercial preparation displayed a homogeneous band on SDS-PAGE and bound two Fe atoms/molecule, it was used as received. Protein was freed from iron and chelating agents by previously reported methods.[11] The resulting apoprotein was used to prepare the diferric and monoferric transferrins preferentially loaded at either the N- or C-terminal sites with ^{56}Fe (as $Fe(NH_4)_2(SO_4)_2 \cdot 6H_2O$ in 1 mM HCl) or ^{57}Fe (as $^{57}Fe_2O_3$ in 6 N HCl).[12,13] After iron loading, all samples were dialyzed against two changes of Hepes buffer (0.05 M Hepes and 0.1 M KCl (pH 7.4)) and concentrated in a collodion membrane ultrafiltration apparatus (Schleicher and Schuell). Samples were transferred to Wilmad precision EPR tubes and stored at liquid nitrogen temperature. Purity of the monoferric preparations was verified by urea gel electrophoresis[11] (Figure 1).

The pure meso isomer of EHPG was the generous gift of Dr. Carl Carrano. Samples for EPR spectroscopy were prepared by adding the ligand to a solution of $FeCl_3$ obtained from 99.9% pure iron wire or 95.6% ^{57}Fe metal. Complete dissolution of the EHPG was attained by adjustment to pH 0.8 with HCl and addition of a slight molar excess of Fe(III). Samples were then brought to 1 mM EHPG, 2 mM $NaClO_4$, 50 mM Hepes, and 100 mM KCl (pH 7.4). The complex gave a single band by thin-layer chromatography, in contrast to the two bands obtained from commercial EHPG (Sigma).

Reagents. Isotopically enriched $^{57}Fe_2O_3$ (90.68%) was supplied by Oak Ridge National Laboratory; ^{57}Fe metal was from Isotec. Other reagents were of the highest grade obtainable. To minimize contamination by extraneous metal ions, all buffers were treated with Chelex 100. Glassware and electrophoresis apparatus were rendered iron free by soaking in 4 N HNO_3 followed by extensive washing with doubly distilled deionized water.

Spectroscopy. EPR spectra were obtained at 77 K with either an IBM-Bruker ESR 200D-SRC or a Varian E-9 spectrometer with TE_{102} cavities. Wilmad precision EPR tubes were used for all samples.

ENDOR experiments were performed at 2.3 K with a Bruker EN810 ENDOR accessory with a 200-W ENI amplifier and a TM_{110} ENDOR cavity mounted in an Oxford ESR 10 cryostat. Data were obtained with

(10) Patch, M. G.; Simolo, K. P.; Carrano, C. J. *Inorg. Chem.* **1983**, *22*, 2630.
(11) Aisen, P.; Leibman, A.; Zweier, J. *J. Biol. Chem.* **1978**, *253*, 1930.
(12) Zak, O.; Aisen, P. *Biochemistry* **1988**, *27*, 1075.
(13) Thompson, C. P.; Grady, J. K.; Chasteen, N. D. *J. Biol. Chem.* **1986**, *261*, 13128.

0002-7863/89/1511-8613$01.50/0

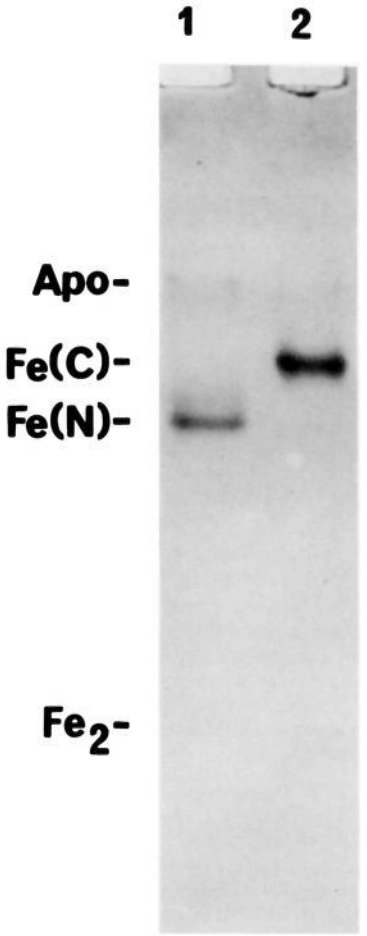

Figure 1. Urea gel electrophoresis of monoferric transferrins, used in the ENDOR studies, selectively loaded at N- and C-terminal sites.

a Bruker 16-turn radio-frequency coil mounted on a cavity insert Dewar. To remove base-line effects and resonances from nuclei other than ^{57}Fe, spectra of ^{56}Fe samples were digitally subtracted from corresponding spectra of ^{57}Fe samples at each magnetic field and for each sample investigated.

Computer programs for analysis of data were written in APL (STSC, Inc.) and executed on an AT-compatible computer.

Experimental Results

ENDOR Spectra of ^{57}Fe–Transferrin Complexes. ENDOR spectra associated with the $g' = 4.3$ EPR line of Fe(III)–transferrin complexes were obtained from both monoferric transferrins as well as from diferric transferrin at fields indicated in Figure 2A. In all cases, the ENDOR lines were centered near 30 MHz, corresponding to a hyperfine splitting of 10 G. This splitting is unresolved in the EPR spectrum of iron-57 transferrin but does result in a noticeable broadening of the $g = 4.3$ line (Figure 2).

ENDOR spectra were obtainable at all fields within the $g' = 4.3$ line (Figures 3–5) and consisted of an envelope of ENDOR resonances about 10 MHz wide. The centers of the envelopes varied with field, ranging from 29 to 32 MHz. Appreciable field dependence in the shapes and frequencies of lines in each envelope was observed, but the overall width of envelopes varied little from field to field for a given complex. In addition to those shown in Figures 3–5, spectra were also recorded at fields of 1560, 1620, and 1624 G. Data from these spectra were included in calculations of spin Hamiltonian parameters. At each field, lines at lowest frequency showed shapes predominantly absorption in character. Although absorption line shapes may suggest passage effects in spectra obtained with frequency-modulated rf and phase-sensitive detection, the shapes were invariant to reduction of rf power and to lowering of modulation depth to 25 kHz. Presumably, therefore, the absorption shapes represent edges of envelopes of unresolved powder lines rather than lines distorted by passage effects.

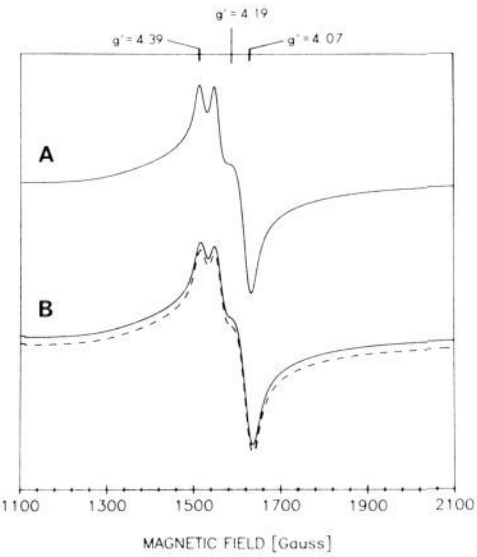

Figure 2. X-band EPR spectra of diferric transferrin bearing naturally abundant iron (A) and isotopically enriched in ^{57}Fe (B). The computer-derived spectrum (dashed lines) represents a 10 G isotropic broadening of line A. Experimental conditions: microwave frequency, 9.299 GHz; microwave power, 10 mW; modulation amplitude, 10 G; modulation frequency, 100 kHz; time constant, 1 s; scan time, 100 s; and sample temperature, 77 K.

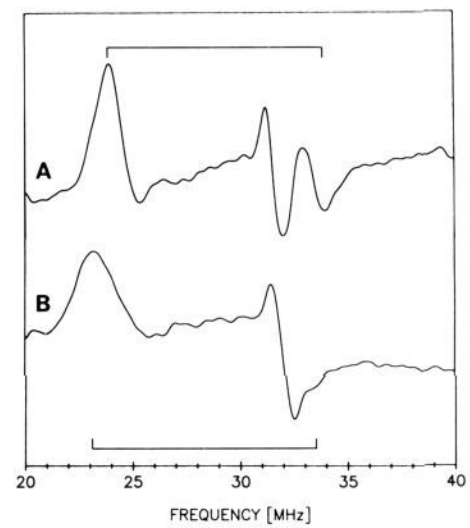

Figure 3. ^{57}Fe ENDOR spectra, taken at the $g' = 4.07$ feature of 1.4 mM N-terminal monoferric transferrin (A) and 1.2 mM C-terminal monoferric protein (B). In this and subsequent figures, spectra of samples loaded with ^{56}Fe were digitally subtracted from corresponding spectra of ^{57}Fe samples, with appropriate corrections for concentration, to eliminate base-line effects and lines from other than ^{57}Fe nuclei. Peak positions taken in analyzing spectra are indicated by ruled lines in this and subsequent figures. Experimental conditions: magnetic field, 1647 G; microwave frequency, 9.389 GHz; microwave attenuation, 10 dB; time constant, 500 ms; gain, 1.25×10^5; rf modulation frequency, 12.5 kHz; rf attenuation, 12 dB; rf modulation depth, 100 kHz; rf scan rate, 1.33 MHz/s; number of scans, 150; and sample temperature, 2.3 K.

Discussion

Interpretation of Spectra. Transferrin-bound ^{57}Fe has an electron spin of $^5/_2$ and a nuclear spin of $^1/_2$. ENDOR spectra of biologically relevant compounds have most often been treated, however, by first-order perturbation theory applied to $S = {}^1/_2$ systems.[14-16] The analysis pertaining to the $S = {}^1/_2$ case may

(14) Rist, G. H.; Hyde, J. S. *J. Chem. Phys.* **1970**, *52*, 4633.
(15) Hoffman, B. M.; Martinsen, J.; Venters, R. A. *J. Magn. Reson.* **1984**, *59*, 110.

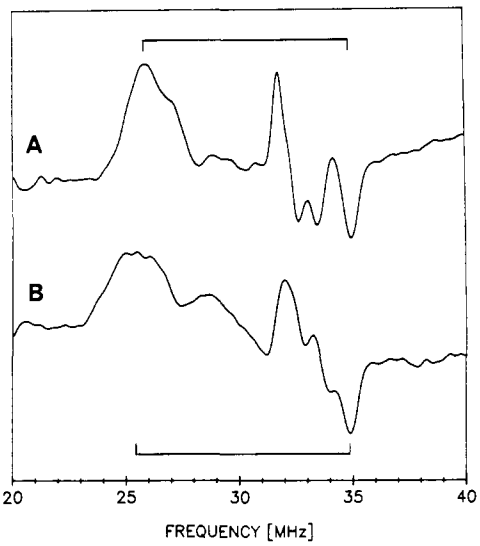

Figure 4. ^{57}Fe ENDOR spectra, at $g' = 4.19$, of N-terminal monoferric transferrin (A) and the C-terminal monoferric protein (B). Magnetic field, 1600 G; other conditions as in Figure 3.

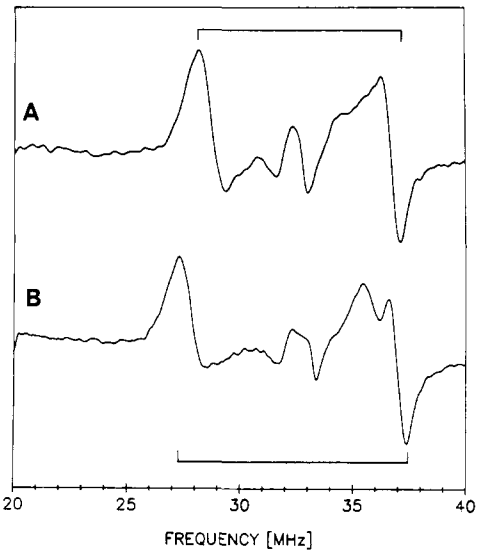

Figure 5. ^{57}Fe ENDOR spectra, at $g' = 4.39$, of N-terminal monoferric transferrin (A) and the C-terminal monoferric protein (B). Digital subtractions were performed as in Figure 3. Magnetic field, 1529 G; other conditions as in Figure 3.

be retained with a minor adjustment for Kramers' systems with $S > {}^1/_2$ if the zero-field splittings are sufficiently large that the Kramers' doublets are effectively isolated from each other. Each Kramers' doublet is then treated as an effective spin ${}^1/_2$ system, with a g value differing from that of the free electron. To first order, the ENDOR frequencies associated with an EPR line are then given by[15,17,18]

$$\nu_{ENDOR} = \frac{g'}{g}\frac{A}{2} \pm \nu_N \quad (1)$$

where g' is the effective g value of the EPR line in which ENDOR transitions are observed, g refers to the free electron g value of 2.00, A is the hyperfine coupling energy, and ν_N is the nuclear Zeeman energy in frequency units. Taking A as 31 MHz, a value obtained by Mössbauer spectroscopy,[19] eq 1 predicts a pair of ^{57}Fe ENDOR frequencies associated with the $g' = 4.3$ signal of iron(III) transferrin centered at 33 MHz and split by the nuclear Zeeman energy, about 0.2 MHz. This splitting is less than the ENDOR line widths, so that only a single ENDOR line is expected, but this is not what is observed (Figures 3–5). Rather, as noted above, a broad envelope of ENDOR lines is found at all field settings within the $g' = 4.3$ EPR signal. Clearly, the g-factor approximation is not adequate to explain the ENDOR spectrum of transferrin-bound Fe(III), and the $S = {}^5/_2$ character of high-spin Fe(III) must therefore be explicitly considered.

The usual spin Hamiltonian is written as

$$\mathcal{H} = D\{\hat{S}_z^2 - {}^1/_3 S(S+1)\} + E\{\hat{S}_x^2 - \hat{S}_y^2\} + g\mu_B \mathbf{B}\cdot\hat{\mathbf{S}} + \hat{\mathbf{S}}\cdot\mathbf{A}\cdot\hat{\mathbf{I}} + g_N\mu_N \mathbf{B}\cdot\hat{\mathbf{I}} \quad (2)$$

where D and E are derived from the traceless fine structure tensor, terms in $\mathbf{S}$ and $\mathbf{I}$ refer to electron and nuclear spins (${}^5/_2$ and ${}^1/_2$, respectively), g is the electronic g value, g_N is the nuclear g value, μ_B and μ_N designate Bohr and nuclear magnetons, $\mathbf{B}$ is the applied magnetic field, and $\mathbf{A}$ is the hyperfine tensor. Operators are indicated by circumflexes, while vector and tensor quantities are given in boldface. Terms in the Hamiltonian have been written in descending order of their contributions to final energies.

The fine structure splittings are substantially greater than energies from other terms,[20,21] so that expressions in D and E are combined and taken as the zeroth-order Hamiltonian. The sum of the electronic Zeeman and hyperfine terms is treated as a perturbation. If the Kramers' doublets lie sufficiently close to each other, a splitting of ENDOR frequencies results that is much larger than the splitting due to the nuclear Zeeman interaction (Figure 6). This field-dependent "pseudonuclear Zeeman effect" (PNZE) is expressed by a second-order correction to energy:[22]

$$\text{PNZE} = \sum_i \left(\frac{\langle 0|\mathbf{A}(\hat{S}\cdot\hat{I})|i\rangle\langle i|g\mu_B(\mathbf{B}\cdot\hat{\mathbf{S}})|0\rangle}{W_0 - W_i} + \frac{\langle 0|g\mu_B(\mathbf{B}\cdot\hat{\mathbf{S}})|i\rangle\langle i|\mathbf{A}(\hat{\mathbf{S}}\cdot\hat{\mathbf{I}})|0\rangle}{W_0 - W_i} \right) \quad (3)$$

Here $\langle 0|$ is a zeroth-order spin state in the middle Kramers' doublet while $\langle i|$ ranges over all the zeroth-order states in the upper and lower doublets. W_0 is the zeroth-order energy of the middle doublet, W_i is the corresponding energy of the upper or lower doublets, and their difference is a zero-field splitting. The operator for the PNZE simplifies to

$$C_x B_x \hat{I}_x + C_y B_y \hat{I}_y + C_z B_z \hat{I}_z \quad (4)$$

the C_i's representing appropriate constants in an expression that has the form of an anisotropic nuclear Zeeman interaction. When the fine structure operator of the spin Hamiltonian lacks a term in E to mix states, the eigenstates of $\hat{S}_z$ and $\hat{I}_z$ serve directly for the calculation of the PNZE.[18,23] In the present case, zeroth-order states for calculation of matrix elements in eq 3 were obtained by numerical diagonalization of the 6×6 matrix of the fine structure Hamiltonian, with values for D (0.30 cm^{-1}) and $|E/D|$ (0.315) representative of those determined by EPR and Mössbauer spectroscopies.[19,21,24] With $\mathbf{A} = 31$ MHz and a field of 1600 G, the calculated PNZE splittings range from 2.9 to 9.8 MHz, depending on the orientation of the fine structure tensor with respect to the external magnetic field.

This anisotropy of the PNZE is a consequence of the anisotropy in apparent g tensors of upper and lower Kramers' doublets. When the field direction is parallel to the X axis of the tensor, taking the Z axis as the axis of quantization in the coordinate system where $|E/D|$ is less than or equal to ${}^1/_3$, the splitting is at a minimum because of the symmetry or near-symmetry in energy

(16) Henderson, T. A.; Hurst, G. C.; Kreilick, R. W. *J. Am. Chem. Soc.* **1985**, *107*, 7299.
(17) Fritz, J.; Anderson, R.; Fee, J.; Palmer, G.; Sands, R. H.; Tsibris, J. C. M.; Gunsalus, I. C.; Orme-Johnson, W. H.; Beinert, H. *Biochem. Biophys. Acta* **1971**, *253*, 110.
(18) True, A. E.; Nelson, M. J.; Venters, R. A.; Orme-Johnson, W. H.; Hoffman, B. M. *J. Am. Chem. Soc.* **1988**, *110*, 1935.
(19) Kretchmar, S. A.; Teixeira, M.; Huynh, B.-H.; Raymond, K. N. *Biol. Met.* **1988**, *1*, 26.
(20) Aasa, R. *J. Chem. Phys.* **1970**, *52*, 3919.
(21) Pinkowitz, R. A.; Aisen, P. *J. Biol. Chem.* **1972**, *247*, 7830.
(22) Abragam, A.; Bleaney, B. *Electron Paramagnetic Resonance of Transition Ions*; Clarendon Press: Oxford, 1970.
(23) Scholes, C. P.; Isaacson, R. A.; Yonetani, T.; Feher, G. *Biochim. Biophys. Acta* **1973**, *322*, 457.
(24) Aasa, R. *Biochem. Biophys. Res. Commun.* **1972**, *49*, 806.

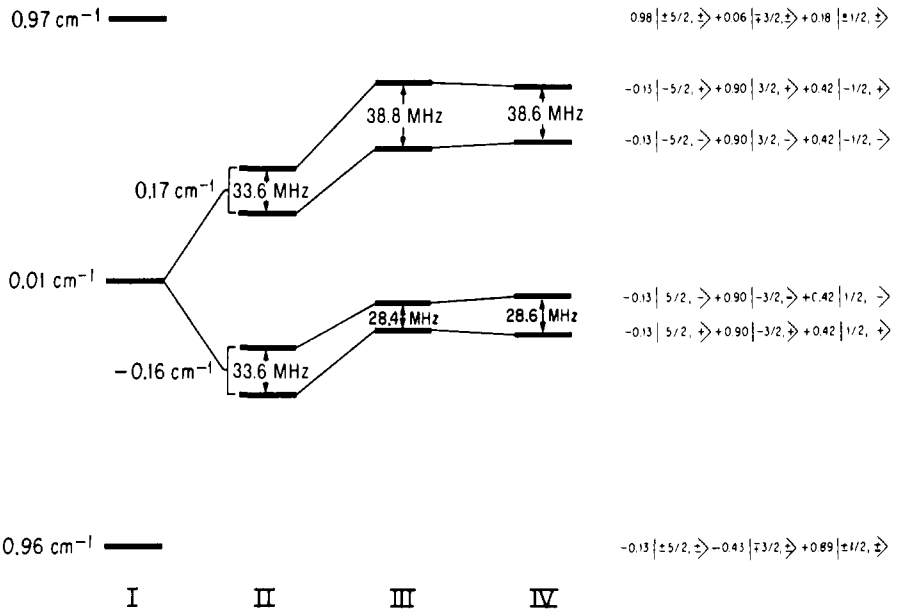

Figure 6. Influence of successive terms of the spin Hamiltonian on energy levels of transferrin-bound Fe(III). (Not to scale.) The Z axis of the zero-field tensor is taken along the external field. The zero-field term (I) leaves a 4-fold degeneracy at each level. The electronic Zeeman and hyperfine interactions break the degeneracy. To first order (II), a single ENDOR line results. In second order (III) an ENDOR splitting occurs. The nuclear Zeeman interaction contributes negligibly (IV). Zeroth-order spin states are tabulated to the right of the energy level diagram. The first label of each state is the z component of electronic spin while the second label refers to nuclear spin. Note that the electronic spin of the upper Kramers doublet is predominantly $\pm^5/_2$, that of the middle doublet $\pm^3/_2$, and that of the lower doublet $\pm^1/_2$. Parameters used in calculations were $D = 0.275$ cm^{-1}, $|E/D| = 0.325$, and $A = 31$ MHz. Energies calculated by the perturbation method differ slightly from those obtained by numerical diagonalization of the full spin Hamiltonian because the fine structure energies are only about three times larger than the electronic Zeeman energies.

Table I. Comparison of ENDOR Splittings from Second-Order Calculation of the PNZE and Numerical Diagonalization of the Spin Hamiltonian[a]

molecular orientation	splitting from 2nd-order perturbation, MHz	splitting from diagonalization of spin Hamiltonian, MHz
X	1.4	1.8
Y	10.2	7.6
Z	10.5	9.7

[a] Parameters used in calculations were $D = 0.275$ cm^{-1}, $|E/D| = 0.325$, $A = 31$ MHz, and $B = 1600$ G.

levels.[21] (The present choice of coordinates differs from earlier usage[21] in that X and Y axes now form a right-handed system.) In the simplest case, $|E/D| = {}^1/_3$, the PNZE would be zero in the X direction since contributions to the PNZE from highest and lowest doublets would be equal in magnitude but opposite in sign thus canceling each other. Splittings in the Y and Z directions, however, would be appreciable and identical, the nonsymmetric energy level diagrams being mirror images of one another in the two directions. In the case of iron(III) transferrin, $|E/D|$ deviates from $^1/_3$ by about 5%. The PNZE splitting will be a minimum but not zero in the X direction, while in the Y and Z directions the splittings would be comparable but not identical (Table I).

The PNZE thus produces an anisotropic ENDOR spectrum with wide splittings even when the **g** and **A** tensors are completely isotropic. The $S = {}^5/_2$ character of iron(III) transferrin and the near-isotropic character of its $g' = 4.3$ line further imply that its ENDOR spectrum should approximate a powder spectrum.[14] This can be appreciated by considering a completely rhombic fine structure tensor ($|E/D| = {}^1/_3$), for which the $g' = 4.3$ EPR line arising from transitions within the middle Kramers' doublet is perfectly isotropic when $D \gg h\nu$.[20] At any point in this line, all orientations of the fine structure tensor with respect to the external field direction would be equally represented. Since ENDOR transitions between states of the middle doublet are intrinsically anisotropic because of the PNZE, the expected result is a powder ENDOR spectrum with line frequencies independent of field along the $g' = 4.3$ EPR line, i.e., a superposition of lines from all orientations with no angle selection effects. Spectroscopic features are then dependent on the functional relation between orientation and ENDOR transitions.[14,15,25] In general, these features are associated with extrema (turning points) of this function. Instances of such turning points would occur when a principal axis of the zero-field tensor is aligned with the external magnetic field and possibly at other orientations as well.[20]

Transferrin-bound Fe(III) represents a case in which the zero-field tensor is not perfectly rhombic, since $|E/D| < {}^1/_3$. As a consequence some angle selection of ENDOR transitions with magnetic field should occur, leading to the field dependence of spectra evident in Figures 3–5. In general, however, considerable superposition of signals arising from different molecular orientations is expected. It is noteworthy that the simplest ENDOR spectrum, Figure 3, was obtained at the low-field limit of the $g' = 4.3$ line where angle selection effects should be greatest. The EPR signal is then dominated by orientations in which the Z axis of the fine structure tensor is aligned with field.[21] In this case the PNZE gives a splitting by second-order perturbation of 11 MHz for the C-terminal site, while the observed splitting (Figure 3B) is 8.9 MHz.

The sensitivity of the PNZE to the zero-field splittings in the denominators of eq 3 makes it possible, to extract values for D and E from analysis of the ENDOR spectra. Parameters in the full-spin Hamiltonian, which maximize concordance between predicted and observed ENDOR frequencies, were found by numerical diagonalization of the 12 × 12 Hamiltonian matrix obtained by taking a basis set of eigenfunctions of $\hat{S}_z$ and $\hat{I}_z$. In these calculations **A** was provisionally treated as a tensor while g was taken as a scalar with a value of 2.0. In the fitting procedure ENDOR frequencies were obtained from the differences in energy of the appropriate eigenstates of the spin Hamiltonian. Initial values of parameters were drawn from previous studies of the EPR and Mössbauer spectra of Fe(III)–transferrin complexes[19,21,24] and were individually adjusted in successive iterations to obtain a least-squares minimization of differences between computed and observed ENDOR frequencies at six field settings. Since experimental ENDOR spectra consist of envelopes of incompletely resolved lines, which we cannot yet simulate and of which only the highest and lowest frequency components can be identified with confidence, these frequencies alone were considered in the

(25) Hurst, G. C.; Henderson, T. A.; Kreilick, R. W. *J. Am. Chem. Soc.* **1985**, *107*, 7294.

Table II. Spin-Hamiltonian Parameters for Fe(III)–Transferrin Complexes

	N-site	C-site
D, cm^{-1}	0.28	0.27
$\|E/D\|$	0.325	0.325
A_x, MHz	31	31
A_y, MHz	30.5	30.5
A_z, MHz	31	31

fitting procedure. Such extrema in frequency arise from orientations in which the Z axis of the fine structure tensor is aligned with the external field. Because of the nearly isotropic character of the $g' = 4.3$ EPR line, angle selection is never complete, so that the Z-orientation is presumably represented at all fields investigated.

An effort was made to include in the spin Hamiltonian quartic terms arising from cubic distortions in the crystal field.[22] These generally resulted in a degradation of fit and so were omitted in the final calculations. Quartic terms are usually small or inconsequential for high-spin Fe(III) and are customarily ignored in the interpretation of EPR and Mössbauer spectra of this species.[20,21,26]

Values of spin Hamiltonian parameters that best fit the experimental data for iron-57 transferrin are presented in Table II. Numerical diagonalization of the 12 × 12 matrix of the complete spin Hamiltonian, with use of these parameters, predicts ENDOR resonances at 28.0 and 29.8 MHz when the X axis of the zero-field tensor is oriented along the external magnetic field of 1600 G, at 25.1 and 32.5 MHz for the Y orientation, and at 25.3 and 35.1 MHz for the Z orientation. Calculations were limited to orientations in which the field direction is parallel to a principal axis of the fine structure tensor. Extrema in splittings are then expected, and these orientations should thus contribute prominently to observed spectra. Other orientations may also contribute spectroscopic features but were neglected at this stage of investigation in order to render computations more tractable. Calculated frequencies then span a range of 9.8 MHz, while the observed envelope of frequencies extends over 9.6 MHz. No attempt was made to simulate the ENDOR powder spectrum since transition probabilities and line shapes are not known.

The spectrum of the C-terminal site corresponding to orientations where alignment of the Z axis of the fine structure tensor with the magnetic field predominates (Figure 3) exhibits an ENDOR splitting of 10.3 MHz. Numerical diagonalization of the spin Hamiltonian predicts a splitting of 9.8 MHz, in somewhat better agreement with observation than the value of 11 MHz obtained from second-order treatment of the PNZE. In general, however, the agreement between ENDOR splittings predicted by numerical diagonalization and those derived from second-order calculations of the PNZE alone (Table I) verify that the PNZE is the major factor contributing to the ENDOR spectrum of the ^{57}Fe(III)–transferrin complex.

Differences between the Two Iron-Binding Sites of Transferrin. The two sites of human transferrin differ in their spectroscopic, thermodynamic, and kinetic properties.[27,28] Differences are also apparent in their ^{57}Fe ENDOR spectra (Figures 3–5). As shown in Table II, these differences are reflected in the "best fit" parameters of the spin Hamiltonian. The N-terminal site is characterized by a slightly larger value of the parameter D than its counterpart, 0.28 versus 0.27 cm^{-1}. Other parameters are indistinguishable for the two sites. Since we are not yet able to simulate ENDOR spectra for a spin $^5/_2$ system with a rhombic fine structure tensor, we cannot further evaluate in detail the basis for the spectroscopic differences between the sites, nor can we relate these differences to known structural differences between the N- and C-terminal domains of transferrin.[29]

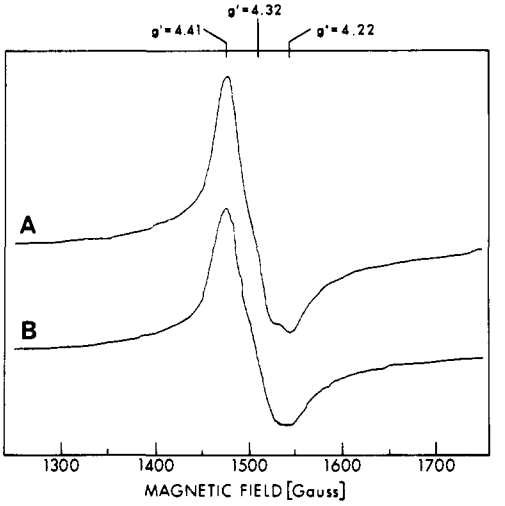

Figure 7. EPR spectra of complexes of the meso isomer of EHPG with naturally abundant iron (A) and ^{57}Fe (B), at pH 7.4. Conditions: microwave frequency, 9.107 GHz; microwave power, 20 dB; modulation amplitude, 10 G; time constant 0.3 s; scan time 2 min; sample temperature, 77 K.

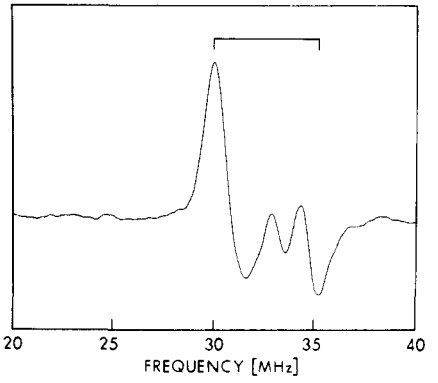

Figure 8. ^{57}Fe ENDOR spectrum of EHPG at $g' = 4.32$ in the EPR spectrum. Rf modulation depth, 200 kHz; other conditions as in Figure 3.

Studies of a Model Compound. ENDOR spectra of ^{57}Fe–EHPG were obtained at fields of 1491.3, 1516.2, and 1583.1 G within the $g' = 4.3$ line of Fe(III)–EHPG (Figures 7 and 8). As with the Fe(III) complexes of transferrin, ENDOR spectra of ^{56}Fe–EHPG were obtained and subtracted from the ^{57}Fe spectra. The ENDOR splittings for ^{57}Fe–EHPG, in the range of 5.1–6.2 MHz, were about half those observed for iron-57 transferrin, indicating that the zero-field splittings, which appear in the denominator of eq 2, must be greater for EHPG than for transferrin. An optimal fit between computer-calculated and experimental frequencies was obtained with $D = 0.76$ cm^{-1}, $|E/D| = 0.31$, and $A_x = A_y = A_z = 29.5$ MHz. Zero-field splittings are thus more than twice those of transferrin. Values for the spin Hamiltonian parameters provided by analysis of the ^{57}Fe ENDOR spectra accord reasonably well with those obtained by Mössbauer spectroscopy, for which values of $|E/D| = 0.28$, $A = 29.3$ cm^{-1} and D ranging from 0.71 to 1.0 cm^{-1} (depending on pH) have been reported.[9] EHPG has been used in the past as a model compound for spectroscopic studies of transferrin.[8] Determination of spin Hamiltonian parameters by ENDOR may extend its usefulness in this respect.

In studies of Cu(II) and Mn(II) complexes, the hyperfine tensor characterizing interaction of the metal ion's electronic moment with its own nucleus has been related to the degree of electron

(26) Scullane, M. I.; White, L. K.; Chasteen, N. D. *J. Magn. Reson.* **1982**, *47*, 383.
(27) Harris, D. C. Aisen, P. *Iron Carriers and Iron Proteins*; Loehr, T. M., Gray, H. B., Lever, A. B. P., Eds.; VCH Publishers: Weinheim, 1989.
(28) Aisen, P. *Iron Carriers and Iron Proteins*; Loehr, T. M., Gray, H. B., Lever, H. B. P., Eds.; VCH Publishers: Weinheim, 1989.
(29) Anderson, B. F.; Baker, H. M.; Dodson, E. J.; Norris, G. E.; Rumball, S. V.; Waters, J. M.; Baker, E. N. *Proc. Natl. Acad. Sci. U.S.A.* **1987**, *84*, 1769.

delocalization from central metal ion to ligands.[30] The hyperfine interaction decreases as electrons are delocalized to ligand orbitals, a feature found particularly useful in interpretation of Cu(II)-protein spectra.[31] ENDOR spectra of bound ^{57}Fe may be comparably valuable in characterizing and understanding high-spin rhombic Fe(III)-protein complexes.

Summary

The feasibility of using ENDOR spectroscopy to study ^{57}Fe hyperfine interactions in rhombic high-spin Fe(III) complexes has been demonstrated. The sensitivity of the ^{57}Fe ENDOR spectrum to fine structure and hyperfine parameters of the spin Hamiltonian shows ENDOR to be a valuable adjunct to CW EPR and Mössbauer spectroscopies in characterizing the properties of biologically significant high-spin Fe(III) complexes. Splitting of lines of an ENDOR pair results from interaction of hyperfine and electronic Zeeman terms in the spin Hamiltonian, the pseudo-nuclear Zeeman effect. Because of the sensitivity of this effect to zero-field splittings, fine structure as well as hyperfine parameters of the spin Hamiltonian may be estimated from the ^{57}Fe ENDOR spectrum.

Acknowledgment. This work was supported in part by Grants 2 RO1 DK15056 (P.A.) and 1 K11 DK01841 (G.A.R.) from the National Institutes of Health.

(30) van Wieringen, J. S. *Discuss. Faraday Soc.* **1955**, *19*, 118.
(31) Vanngard, T. *Biological Applications of Electron Spin Resonance*; Swartz, H. M., Bolton, J. R., Borg, D. C., Eds.; Wiley-Interscience: New York, 1972; pp 411-447.

Electrochemical, Theoretical, and ESR Characterizations of Porphycenes. The π Anion Radical of Nickel(II) Porphycene

M. W. Renner,[1a] A. Forman,[1a] W. Wu,[1b] C. K. Chang,[1b] and J. Fajer*,[1a]

Contribution from the Department of Applied Science, Brookhaven National Laboratory, Upton, New York 11973, and the Department of Chemistry, Michigan State University, East Lansing, Michigan 48824. *Received January 23, 1989*

Abstract: Electrochemical, optical, ESR, ENDOR, and theoretical results are presented for nickel(II) 2,7,12,17-tetrapropylporphycene and its one-electron reduction product. The nickel complex of this novel class of porphyrin isomers was chosen to probe the electronic configurations of porphycenes, to assess the role of the porphycene ligand in controlling sites of reduction (metal versus macrocycle), to determine the effects of its D_{2h} symmetry compared to the D_{4h} symmetry of porphyrins on ESR spectral resolution, and to compare with the reductive chemistry of nickel porphyrins used to model the reactions of F430, the nickel tetrapyrrole found in methanogenic bacteria. Reduction of the Ni(II) porphycene yields a π anion radical whose redox, optical, and ESR characteristics are in good agreement with extended Hückel and ZINDO molecular orbital calculations and thus begin to define the electronic configuration of this new class of porphyrin derivatives.

The seminal syntheses by Vogel and co-workers[2] of porphycenes, the novel porphyrin isomers, led us to investigate the reduction of nickel(II) 2,7,12,17-tetrapropylporphycene (TPrPc, see Figure 1) for several reasons. (1) Little is known about the electronic factors that determine the properties of porphycenes and the consequences of isomerization of the porphynoid structure. (2) The reduction of nickel(II) porphyrin derivatives is being extensively studied to model F430, the nickel tetrapyrrole that catalyzes CO_2 conversion to methane in methanogenesis. Ni(II) radicals and Ni(I) anions have been reported as reduction products.[3-9] (3) Porphycenes are easier to reduce than porphyrins or hydroporphyrins and the relative reordering of the metal and π^* orbitals may therefore yield π anions unambiguously. (4) The D_{2h} symmetry of the porphycenes should remove the orbital degeneracy of the π^* orbitals found in D_{4h} porphyrins that results in a lack of ESR resolution and does not allow direct comparison with molecular orbital calculations.[10,11]

We present here redox, ESR, ENDOR, optical, and theoretical results for the π anion of nickel(II) porphycene that help characterize this novel class of compounds.

Methods

ESR and ENDOR spectra were recorded on a Bruker-IBM ER 200D spectrometer equipped with an ER 251 double resonance system, a field frequency lock, and an Aspect 2000 data acquisition system. NMR spectra were obtained in $CDCl_3$ at 250 MHz on a Bruker WM-250 instrument. Mass spectra were measured on a JEOL HX 110 spectrometer. Optical spectra were recorded on a Cary 2300 spectrophotometer. Anion radicals were generated electrochemically in tetrahydrofuran (THF) at Pt electrodes in vacuo.[12] ESR samples were equipped with optical cells to allow monitoring before and after the ESR measurements.[12] Cyclic voltammograms were obtained in CH_2Cl_2 in a microcell[13] under a N_2 atmosphere relative to a SCE electrode. THF and CH_2Cl_2 were distilled from CaH_2. The THF was degassed by freeze-

(1) (a) Brookhaven National Laboratory. (b) Michigan State University.
(2) Vogel, E.; Köcher, M.; Schmickler, H.; Lex, J. *Angew. Chem., Int. Ed. Engl.* **1986**, *25*, 257. Vogel, E.; Balci, M.; Pramod, K.; Koch, P.; Lex, J.; Ermer, O. *Angew. Chem., Int. Ed. Engl.* **1987**, *26*, 928.
(3) Ellefson, W. L.; Whitman, W. B.; Wolfe, R. S. *Proc. Natl. Acad. Sci. U.S.A.* **1982**, *79*, 3707. Hausinger, R. P.; Orme-Johnson, W. H.; Walsh, C. *Biochemistry* **1984**, *23*, 801. Daniels, L.; Sparling, R.; Sprott, G. D. *Biochim. Biophys. Acta* **1984**, *768*, 113. Fässler, A.; Kobelt, A.; Pfaltz, A.; Eschenmoser, A.; Bladon, C.; Battersby, A. R.; Thauer, R. K. *Helv. Chim. Acta* **1985**, *68*, 2287 and references therein.
(4) Albract, S. P. J.; Ankel-Fuchs, D.; Van der Zwaan, J. W.; Fontjin, R. D.; Thauer, R. K. *Biochim. Biophys. Acta* **1986**, *870*, 50.
(5) Jaun, B.; Pfaltz, A. *J. Chem. Soc., Chem. Commun.* **1986**, *1327*.
(6) Stolzenberg, A. M.; Stershic, M. T. *Inorg. Chem.* **1987**, *26*, 1970; *J. Am. Chem. Soc.* **1988**, *110*, 6391 and references therein.
(7) Renner, M. W.; Forman, A.; Fajer, J.; Simpson, D.; Smith, K. M.; Barkigia, K. M. *Biophys. J.* **1988**, *53*, 277.
(8) Lexa, D.; Momenteau, M.; Mispelter, J.; Saveant, J. M. *Inorg. Chem.* **1989**, *28*, 30.
(9) Kadish, K. M.; Sazou, D.; Maiya, G. B.; Han, B. C.; Liu, Y. M.; Saoiabi, A.; Ferhat, M.; Guilard, R. *Inorg. Chem.* **1989**, *28*, 2542.
(10) (a) Fajer, J.; Davis, M. S. In *The Porphyrins*; Dolphin, D., Ed.; Academic Press: New York, 1979; Vol. 4, p 197. (b) Felton, R. H. In *The Porphyrins*; Academic Press: New York, 1978; Vol. 5, p 53.
(11) Schlüpmann, J.; Huber, M.; Toporowicz, M.; Köcher, M.; Vogel, E.; Levanon, H.; Möbius, K. *J. Am. Chem. Soc.* **1988**, *110*, 8566.
(12) Fajer, J.; Fujita, I.; Davis, M. S.; Forman, A.; Hanson, L. K.; Smith, K. M. *Adv. Chem. Ser.* **1982**, *201*, 489.
(13) Fujita, I.; Chang, C. K. *J. Chem. Educ.* **1984**, *61*, 913.

0002-7863/89/1511-8618$01.50/0